N86-27201

VORTEX FLOW HYSTERESIS

Atlee M. Cunningham, Jr.
General Dynamics
Fort Worth Division
Fort Worth, Texas

SUMMARY

An experimental study was conducted to quantify the hysteresis associated with various vortex flow transition points and to determine the effect of planform geometry. The transition points observed consisted of the appearance (or disappearance) of trailing-edge vortex burst and the transition to (or from) flat plate or totally separated flows. Flow visualization with smoke injected into the vortices was used to identify the transitions on a series of semi-span models tested in a low-speed tunnel. The planforms tested included simple deltas (55 deg to 80 deg sweep), cranked wings with varying tip panel sweep and dihedral, and a straked wing. High-speed movies at 1000 frames per second were made of the vortex flow visualization in order to better understand the dynamics of vortex flow, burst and transition.

INTRODUCTION

Recent interest in flying at very high angles of attack beyond the static stall conditions has been kindled by proposals to exploit this flow regime to improve fighter aircraft maneuverability (refs. 1 and 2). Herbst's concept to fly into the post-stall regime to achieve quicker turns (ref. 1) and the use of unsteady aerodynamics at high incidence discussed by Lang and Francis (ref. 2) open a Pandora's box of new aerodynamic problems. Because these ideas require flying at incidences as high as 90 deg or beyond, a single maneuver could cover vortex and burst vortex flows as well as totally separated flows. Also, because of the maneuver dynamics, pitch rate and time history effects could be very important. The understanding of these flow fields and the dynamic effects represents a quantum jump over current aerodynamic technology. Thus, as a first step toward this goal, a need exists to identify the various flow regimes and their characteristics as well as transition points from one type to another and the associated hysteresis effects.

The upper surface flow fields that exist over slender, highly swept or straked wings at high angles of attack may take on various forms. These forms may be broadly classified as three types summarized in Figure 1:

(1) Vortex flows (stable leading edge or strake vortex)
(2) Burst vortex flows (unsteady but still vortical)
(3) Flat plate flows (unsteady, completely separated)

The normal force curve slope for type 1 flows is quite high compared to that of the attached flow region which generally exists below 5 deg. to 8 deg. incidence as illustrated in figure 1. The slope is reduced once vortex bursting begins to occur over the wing but normal force still increases with increasing incidence. Once the flow breaks down to the final stage of flat plate flow, normal force remains about constant, even up to 90 deg. incidence. The transition to flat plate flow is generally quite abrupt and may be accompanied by a loss in normal force or a destabilizing change in pitching moment with increasing incidence. Another very important property of these transitions is the hysteresis effect that results from transitions occurring at different incidences depending on whether the angle is increasing or decreasing. Quantification of this hysteresis and the determination of the effect of planform geometry on its characteristics are the objectives of this paper.

In order to accomplish these objectives, an experimental program was conducted in which a series of delta and cranked flat plate wings were tested. Flow visualization techniques were used to determine the transition points and the associated hysteresis. The tests were conducted in a small low speed tunnel at General Dynamics' Fort Worth Division using smoke for the flow visualization. The smoke generator was a special design that was evolved at General Dynamics for testing vortical flows at very high incidence. The models were semi-span models cut from flat aluminum plate with rounded leading edges. The planforms tested included simple deltas, cranked wings with varying tip panel sweep, a cranked wing with varying tip panel dihedral, and a straked wing. Data taken during the test for increasing and decreasing incidence included angles of the appearance of vortex burst at the wing trailing edge and transition to or from flat plate flow. High speed movies were made of the vortex flows to reveal the spiral nature of vortex burst and other unsteady phenomena.

TEST SETUP AND PROCEDURE

The small continuous low speed wind tunnel at General Dynamics' Fort Worth Division was used for this investigation. The tunnel has a $0.356 \times 0.356 m^2$ (14×14 in.^{2}) test section with a splitter plate installed on one wall and clear glass on the other three walls for viewing flow visualization experiments. Test velocities used were held approximately constant at 30m/sec (98 ft/sec) which previous experience has shown to yield reliable vortex flow characteristics and good flow visualization using smoke.

The semi-span models were cut from flat aluminum plate stock, 0.160 cm (0.063 in) thick, and mounted on a bracket attached to a shaft extending outside the tunnel as shown in figure 2. Angle of incidence was set by rotating the shaft which was attached to a calibrated plate with angle marks. The settings were made manually so that very slow and smooth approaches to flow transition points could be achieved. Angle readings were made visually and recorded by hand.

The smoke generator was also installed on the wing mounting bracket as shown in figure 2 to permit injection of smoke as close as possible to the nose so as to provide maximum visualization of the leading-edge vortex. The smoke generator consisted of 0.05 cm ID (0.02 in.) stainless-steel tubing through which kerosene was forced from a pressurized vessel as shown in figure 3. A 23 cm (9 in.) section of the tubing near the nozzle was heated with DC current at about 10 amps. The heated kerosene vaporized when it exited from the nozzle in a reasonably steady flow. Pulsation was minimized by adjusting current and kerosene flow.

The semi-span models tested are shown in figure 4 with specifications listed in table 1. The leading edges were rounded such that they were semi-circular with a diameter of the thickness of the plate, 0.160 cm (0.063 in.). This was done to avoid adding any leading-edge camber that would result from having a sharp edge with a flat upper surface and also to simplify model fabrication. The cranked wing planforms all had a common inboard leading-edge sweep of 70 deg with the crank placed at 70% span. Only the tip panel sweep was varied from 30 deg to 70 deg and the tip panel dihedral varied from -90 deg to +90 deg with a fixed tip sweep of 30 deg. The straked wing planform was tested to provide insight as to the character of strake flows as opposed to simple delta and cranked wings. All sweep and dihedral were measured and recorded after fabrication.

The test procedure was very simple once the optimum conditions for smoke visualization were established. The wings were attached to the mounting bracket, the tunnel started, then the smoke turned on. The test was conducted on a continuous basis for each wing. The determination of transition angles was made as an average of at least three observations for each point. For increasing incidence, the angle was always lowered far below the transition point and then slowly increased until the transition occurred. For decreasing incidence, the reverse procedure was followed. In all cases fully established flow was obtained just before transition.

Calibration of test set-up was accomplished by comparing measured transition points with existing data for planforms of similar geometries. The items checked were wall interference and gap between the splitter plate and model root chord. Wall interference was about 10% at an incidence of 45 deg for the cranked wings and the delta wings for an incidence less than 70 deg. To check this effect, the angle for trailing-edge burst was compared with data published in

reference 3. This comparison shown in figure 5 indicates that the correlation is quite good. Another check on interference was a qualitative assessment of vortex burst development downstream of the model. Progression of the burst point toward the wing was very uniform and controllable with wing incidence.

The idea of leaving a small gap between the splitter plate and wing root chord was to prevent contamination of the vortex development by the wall boundary layer. This problem is unique to semi-span testing. The gap was set at the estimated displacement thickness of the wall boundary layer, 0.16 cm (1/16 in.). Variation of this gap to zero was shown to have little effect on the trailing-edge (TE) vortex burst angle but a profound effect on the transition to flat plate (FP) flow. Data available from a large-scale full span low-speed test of a General Dynamics research model similar to the 70 deg/50 deg cranked wing indicated that the transition to FP flow should occur at about 43 deg - 47 deg incidence. With the gap set at 0.16 cm, this transition occurred at about 45 deg - 46 deg but with zero gap, it occured at about 55 deg - 60 deg. Therefore the gap was maintained at the 0.16 cm value for all models tested.

RESULTS AND DISCUSSION

The objective of this test was to quantify the hystereses associated with various vortex flow transition points and determine the effect of planform geometry on their characteristics. The transition points observed consisted of the appearance (or disappearance) of trailing-edge (TE) vortex burst and transition to (or from) flat plate (FP) flows. Flow visualization with smoke injected into the vortices was used to identify the transitions that occurred over a series of flat plate models that included a set of deltas, a cranked wing with varying tip panel sweep or dihedral, and a straked wing (see fig. 4). Finally, high-speed movies were made to reveal the spiral nature of vortex breakdown and other dynamic effects.

Transition Points and Hysteresis

The results for TE vortex burst on the delta wings already discussed in the previous section are shown in figure 5. Shown also in the figure are data from other sources (reference 3) that indicate good agreement with the present data. Hysteresis could not be detected during the test for the TE vortex burst; in fact, when the angle was held steady at the TE vortex burst point, the burst would slowly move back and forth with a range of only about 5% of the wing root chord. TE vortex burst for the delta wings was highly stable.

Results for FP flow transition for the delta wings are shown in figure 6. The influence of sweep is similar to that for the TE vortex burst angle in figure 5; however, a definite hysteresis effect is present. Amplitude of the hysteresis is about constant at 3 to 4 deg for all sweeps with the exception of 70 deg which is only about 2 deg. These points were re-checked for several wings but results were still the same. A possible explanation is that it appears that vortex assymmetry develops in the incidence range of 45 deg for 70 deg delta wings (ref. 4). If this is the case, then the higher swept wings would also be in the asymmetric vortex range and semi-span testing which enforces symmetry of these models could be questionable. Although this subject requires further investigation with full span models, it is felt that the hysteresis trends as a function of wing sweep are reasonable because the variation over the test range is orderly and closely parallels that of TE vortex burst.

The influence of tip sweep angle on TE vortex burst for the cranked wing with 70 deg inboard sweep is shown in figure 7. The reduction of hysteresis with increasing tip sweep was expected. It is interesting that the maximum angle for increasing incidence was very close to that of the simple 70 deg delta wing at 29 deg and is essentially independent of tip sweep. A more interesting observation, however, is that when TE burst appeared, it would not occur at the trailing edge - instead it would develop with the usual orderly upstream progression on the wake vortex and upon reaching the trailing edge would immediately jump forward to a point just upstream of the axial location of the wing crank (approximately 79% of the root chord). When vortex burst reached the trailing edge with decreasing incidence, however, it did so in an orderly fashion as observed for the delta wings but then jumped from the trailing edge to a point further downstream as it passed the trailing edge.

The observed hysteresis of TE vorex burst on the cranked wings is attributed to flow conditions on the tip panel just prior to TE vortex burst. With increasing incidence, the tip panel flow fields are well behaved and dominated by the inboard panel leading-edge vortex; hence, forward progression of burst in the wake is fairly insensitive to the tip panel presence or geometry. When burst reaches the trailing edge, the tip upper surface flow field suddenly collapses with a resulting rise in pressure that forces burst to abruptly move forward of the wing crank axial location. With decreasing incidence, the opposite process takes place. In this case the lower sweep panel does not re-establish its flow as quickly because its starting point is burst vortex flow. Aft progression of the burst with decreasing incidence is similar to that of a lower swept wing. For example, TE vortex burst for decreasing incidence on the cranked wing with tip sweep of 30 deg occurs at about 21 deg as shown in figure 7. This compares favorably with the angle of TE vortex burst for a delta wing with a sweep of about 64 deg as shown

in figure 5. Upon reaching the trailing edge, however, the tip panel flow fields are then fully re-established and the burst must jump abruptly downstream to a point corresponding to that which would occur during the case of increasing incidence but at the lower angle of attack.

A second variation of tip panel geometry which affects TE vortex burst hysteresis is tip panel dihedral. Results for this investigation, shown in figure 8, indicate that changing the dihedral with a fixed tip sweep of 30 deg has a profound effect on the hysteresis. In general, positive dihedral reduces hysteresis from 8 deg at zero to 0.5 deg at 45 deg. At 60 deg dihedral, the hysteresis has disappeared and the TE vortex burst point angle has increased to 30 deg. A further increase to 90 deg dihedral results in a drop of TE vortex burst angle to 27.5 deg but has not introduced any hysteresis.

Negative dihedral for -30 deg to -90 deg shows a large reduction in hysteresis but it also shows a reduction in TE vortex burst angle to an average of about 26 deg for all dihedral angles. The reasons why tip dihedral has these effects on TE vortex burst are not clear; however, several possibilities will be discussed.

Changing of the tip panel dihedral does at least two things: (1) it changes the leading-edge sweep with angle of attack, and (2) it changes the orientation of the tip leading edge relative to the local upwash fields, ie., positive dihedral leads to a more spanwise flow whereas negative dihedral leads to a more perpendicular or two dimensional flow. With positive dihedral, these two changes tend to improve the tip panel flow fields at higher angles of attack; hence, with increasing dihedral, the hysteresis disappears. In the case of 60 deg dihedral, the TE vortex burst angle was actually increased over that of the 70 deg delta. Going too far, however, to 90 deg results in adverse effects which lower the TE vortex burst angle but still do not introduce any hysteresis. At this high dihedral, the spanwise flow must make an abrupt turn when it encounters the vertical tip panel and hence a corner vortex forms that precipitates premature burst of the main wing vortex. With exception of the 90 deg dihedral, the main vortex structure and path seemed to be little affected by the dihedral.

Negative dihedral has the interesting effect of lowering the TE vortex burst angle but also reducing the hystesis. In fact, this dihedral direction was more effective at reducing hystesis than positive dihedral. It is suspected, however, that the reduction in hysteresis was bought at the price of premature separation of the tip panel due to both decreased sweep and higher upwash angles at the leading edge. Therefore, it appears that configuration designs based on cranked wings with large negative tip dihedrals would not be very efficient at high angles of attack.

The transition to and from FP flows for the cranked wings was found to be relatively unaffected by the wing tip geometry. Results shown in figure 9 indicate the influence of tip panel sweep on the FP flow transition. Hysteresis amplitudes and the angles show very little variation, in fact 30 deg and 70 deg have identical values. Data obtained for tip dihedral effects also exhibited the same characteristic and hence are not shown. The reasons attributed to this observation are based on the fact that the large inboard part of the cranked wing is the dominant geometric feature that governs the flow fields near FP flow transition. Thus, radical changes in the small tip have very little effect on this transition.

The straked wing shown in figure 4 represents a variation of cranked wing planforms where the outboard "tip" panel is dominant. This wing was tested because: (1) it is representative of the F-16 planform, and (2) a force and pressure model of this same geometry will be tested at a later date by General Dynamics. High-speed movies were also made of the vortex flow visualizations for this model which will be discussed in the next subsection. Test results for the straked wing were:

TE vortex burst	= 18 deg increasing incidence
FP flow transition	= 48 deg increasing incidence
FP flow transition	= 43.5 deg decreasing incidence
TE vortex burst	= 18 deg decreasing incidence

For a strake sweep of 76 deg, the delta wing TE vortex burst angle would be about 34 deg as shown in figure 5. In the presence of the large outboard 40 deg panel, this was reduced to 18 deg which illustrates the effect increasing the tip panel size for cranked wing geometries. In the case of the cranked wings discussed earlier, the observation that TE vortex burst angle for increasing incidence was little affected by tip sweep or positive dihedral was attributed to small tip panel size. In that case, the inboard panel vortex dominated the outboard panel flow fields prior to burst. For the straked wing, earlier breakdown of the large outboard panel due to lower sweep led to early breakdown of the strake vortex. The FP flow transition angle was likewise reduced to 43.5 - 48 deg from the range of about 52 - 55 deg shown in figure 6 for a 75 deg delta wing. The idea of straked wing designs, however, is not to achieve the high incidence characteristics of the strake but to extend the incidence range of lower swept higher aspect-ratio wings which have better efficiencies than highly swept delta wings (refs. 5 and 6).

The absence of hysteresis for TE vortex burst on the straked wing is puzzling but the 4.5 deg amplitude for FP flow transition is in line with those amplitudes shown in figure 6. The angle for TE vortex burst of 18 deg correlates quite well with the observed lift curve break at 18 deg for the YF-16 at low speeds (ref. 6); therefore, the basic flow field properties are probably correct. A possible explanation is that the outboard panel exhibits orderly growth of trailing-edge separation and since it dominates the strake, the

strake vortex likewise bursts in an orderly fashion. In this case the outboard panel dominates for both increasing and decreasing incidence and hence little or no hysteresis appears in the TE vortex burst point. For the case of the cranked wings discussed earlier, the hysteresis was a result of differing dominance with incidence direction; with increasing incidence, the inboard panel leading-edge vortex dominated the tip panel flow fields, and with decreasing incidence, the separated flow on the wing tip dominated itself.

High-Speed Movie Results

High-speed movies at 1000 frames per second were made of the vortex flow visualization in order to better understand the dynamics of the unsteady separated flows. A schematic of the flow visualization is shown in figure 10 to orient the reader with the photos to be discussed. These discussions will be based on conclusions arrived at from viewing the movies, thus the writer will verbally add the dynamic effects to the individual frames taken from the movies.

The frames shown in figure 11 are taken from a high-speed movie made of a slow pitch sweep up to 55 deg incidence for the straked wing that was just discussed in the previous subsection. The only difference between the movie configuration and that above was the flat extension just aft of the wing as noted in figure 10. At about 15 deg (figure 11a) the strake vortex is about to burst as noted by a kink that developed just aft of the trailing edge. At about 20 deg (figure 11b) the vortex has burst and the movie is already showing the swirling pattern associated with spiral burst. Also, in the movie it is evident that significant spanwise flow outboard along the trailing edge is occurring which is attributed to trailing-edge separation as discussed previously for the straked wing. At about 28 deg (figure 11c) the burst has progressed to a point just aft of the wing/strake intersection. The spiral vortex breakdown as well as the spanwise trailing-edge flow are now more evident. At about 35 deg (figure 11d), the burst has moved forward and developed further but is similar in appearance to that at 28 deg. At about 45 deg (figure 11e), the outer wing panel has transitioned to FP flow as indicated by absence of smoke over that region. As shown in the movie, this transition was very abrupt. At about 55 deg (figure 11f), the flow picture has not changed much from that at 45 deg. In both figures 11e and 11f, the strake flow forward of the outboard panel leading edge is completely burst but still vortical.

Figure 12 shows a similar sequence of frames taken from a high-speed movie made of a slow pitch sweep up to about 60 deg for a cranked wing with 68.5 deg/21.5 deg leading-edge sweeps. The wing planform, also shown in figure 12, is similar to but slightly different than that discussed in the previous subsection of this paper. Nevertheless, the basic flow field characteristics are similar. At

about 20 deg (figure 12a) the vortex is well formed. Burst occurs at about 24-25 deg as shown in figure 12b which correlates well with the data in figure 5 for a 68.5 deg swept delta. The burst is located just forward of the wing crank right after its initial appearance. The high-speed movie shows a very rapid movement of the burst from the trailing edge to the point shown in figure 12b which is part of the hysteresis mechanism discussed previously. At about 35 deg (figure 12c) the burst has further developed and is very close to the wing vertex. This frame very clearly shows the spiral vortex burst. At about 45 deg (figure 12d) the vortex is completely burst but the flow is still vortical just prior to FP flow transition. At about 55 deg (figure 12e) FP flow, or total separation, is shown for which the transition occurred very abruptly at about 46-47 deg. During the reverse pitch sweep back to zero incidence as shown in the movie, hysteresis for the FP flow transition is not as clear as that for TE vortex burst. The angle for the TE vortex burst with decreasing incidence is about 16-17 deg, thus the hysteresis amplitude of about 8-9 deg can be easily detected in the movie. Also, the different speed of vortex burst movement near the trailing edge for increasing and decreasing incidence is clearly evident.

The high-speed movies of vortex flow visualization have provided valuable insight to the dynamics of vortex flows, burst, and transitions. With a shutter speed of 1/3000 sec at 1000 frames per second and flow velocities of about 30 m/sec, the spiral motion of vortex burst was stopped. Vortex burst movement on the cranked wing during initial development was slowed down to show that even though the development was very rapid, it was orderly. Also spanwise trailing-edge flow during vortex burst on the straked wing was shown to be a possible explanation for the absence of TE vortex burst hysteresis for that wing. FP flow transitions were shown to be very rapid for all wings for either increasing or decreasing incidence.

CONCLUDING REMARKS

An experimental study was conducted to quantify the hysteresis associated with various vortex flow transition points and determine the effect of planform geometry on their characteristics. The transition points observed consisted of the appearance (or disappearance) of trailing-edge (TE) vortex burst and transition to (or from) flat plate (FP) flows. Flow visualization with smoke injected into the vortices was used to identify the transitions that occurred on a series of semi-span models tested in a low-speed wind tunnel at about 30m/sec. The planforms tested consisted of simple deltas (55 to 80 deg sweep), cranked wings with varying tip panel sweep and dihedral,

and a straked wing. High-speed movies at 1000 frames/sec were made of the vortex flow visualization in order to better understand the dynamics of vortex flow and burst as well as the transition from one flow type to another.

Results were obtained for the hysteresis characteristics of both TE vortex burst and FP flow. Delta wings were first tested for a series of leading-edge sweeps of 55, 60, 65, 70, 75 and 80 degrees. TE vortex burst angles were determined and good correlation with other published data verified the test setup and procedure; however, little or no hysteresis was observed. Particular attention was paid to the semi-span test techniques. FP flow transition angles were found to increase with leading-edge sweep in much the same way as TE vortex burst; however, a hysteresis was observed which was constant at about 3-4 deg. This transition consistently occurred at higher angles for increasing incidence than for decreasing incidence.

Test results for the cranked wings exhibited very interesting effects of tip panel geometry on the hysteresis characteristics. For a fixed inboard sweep of 70 deg, varying the outboard sweep from 30 to 70 deg showed a reduction of TE vortex burst hysteresis from 8 deg at 30 deg sweep to 0 deg at 60 deg and 70 deg sweeps. Varying tip panel dihedral from -90 to +90 deg for the 70 deg/30 deg cranked wing also showed a reduction of TE vortex burst hysteresis. For dihedral varying from 0 to 90 deg, the hysteresis was reduced from 8 deg at 0 deg dihedral to 0 deg at 60 deg dihedral where the angle for TE vortex burst was also slightly increased. At 90 deg dihedral, the hysteresis was zero; however, the TE vortex burst angle was lowered significantly. For negative dihedral, the hysteresis was again reduced, but the TE vortex burst angle was consistently lower for all values. The influence of tip panel geometry was found to be insignificant for the transition to FP flows. This characteristic was about the same as that for the 70 deg delta.

The straked wing tested with 76 deg/40 deg leading-edge sweep was similar to an idealized F-16 and represented a variation on cranked wings where the outboard panel was the dominant surface. The absence of TE vortex burst hysteresis was attributed to the orderly development of trailing-edge separation on the 40 deg panel as observed in the high-speed movies. Hysteresis was observed for FP flow transition and was associated with total separation of the 40 deg panel. This separation was observed in the high-speed movies to be very abrupt.

The high-speed movies provided valuable insight to the dynamics of vortex flows, burst and transition. The spiral motion of vortex burst was stopped and the very rapid initial movement of the burst point on the cranked wings was shown to have an orderly development. Spanwise flow along the trailing edge for vortex burst on the straked

wing was shown to be a possible explanation for the absence of TE vortex burst hysteresis for that wing. Finally, the transition to FP flow was found to be very abrupt, even at 1000 frames/secs for all wings for either increasing or decreasing incidence.

REFERENCES

1. Herbst, W. B.: Dynamics of Air Combat., J. Aircraft, vol. 20, No. 7, July 1983, pp. 594-598.

2. Lang, J. and Francis, M. S.: Unsteady Aerodynamics and Dynamic Aircraft Maneuverability. Presented at AGARD Symposium on Unsteady Aerodynamics - Fundamentals and Applications to Aircraft Dynamics, Gottingen, Germany, 6-9 May 1985, Paper No. 29.

3. Malcom, G. N.: Impact of High-Alpha Aerodynamics on Dynamic Stability Parameters of Aircraft and Missiles. AGARD-LS-114, 1981.

4. Ericsson, L. E.: Wing Rock Flow Phenomena. Presented at AFOSR/FJSRL/U. Colorado Workshop on Unsteady Separated Flows, USAF Academy, 10-11 August 1983.

5. Peake, D. J. and Tobak, M.: On Issues Concerning Flow Separation and Vortical Flows in Three Dimensions. AGARD-CP-342, 1983, Paper No. 1.

6. Smith, C. W., Ralston, J. N. and Mann, H. W.: Aerodynamic Characteristics of Forebody and Nose Strakes Based on F-16 Wind Tunnel Test Experience. NASA CR-3053, 1979.

TABLE 1 Model Specifications

Root Chord, cm	Leading Edge Sweep, Deg	Tip Panel Sweep, Deg	Tip Panel Dihedral, Deg	Location of Crank, % Span
DELTA WINGS				
22.9 cm	55°	-	-	-
25.4 cm	60°	-	-	-
27.9 cm	65°	-	-	-
30.5 cm	70°	-	-	-
↓	75°	-	-	-
	80°	-	-	-
CRANKED WINGS				
30.5 cm	70°	30°	0°	70%
↓	↓	40°	↓	↓
		50°		
		60°		
30.5 cm	70°	30°	-89°	70%
↓	↓	↓	-60°	↓
			-46.5°	
			-30°	
			15°	
			31°	
			46°	
			90°	
STRAKED WING				
26 cm	76°	40°	0°	25%

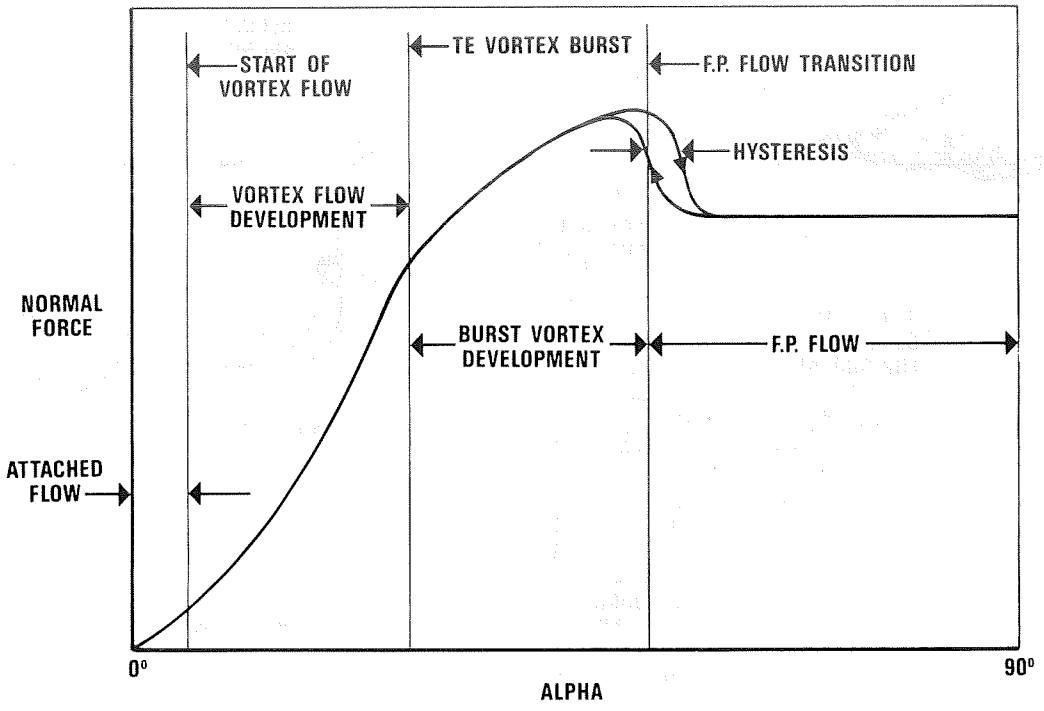

Figure 1 Regimes of Vortical Flow Development.

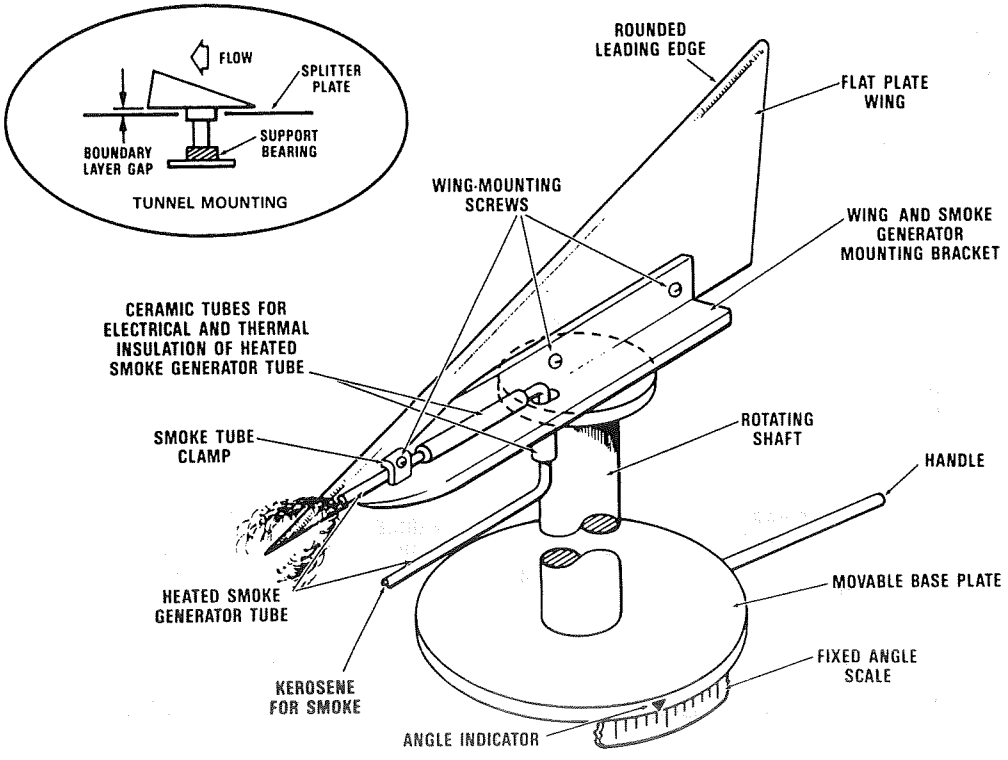

Figure 2 Schematic View of the Semi-Span Model Test Assembly.

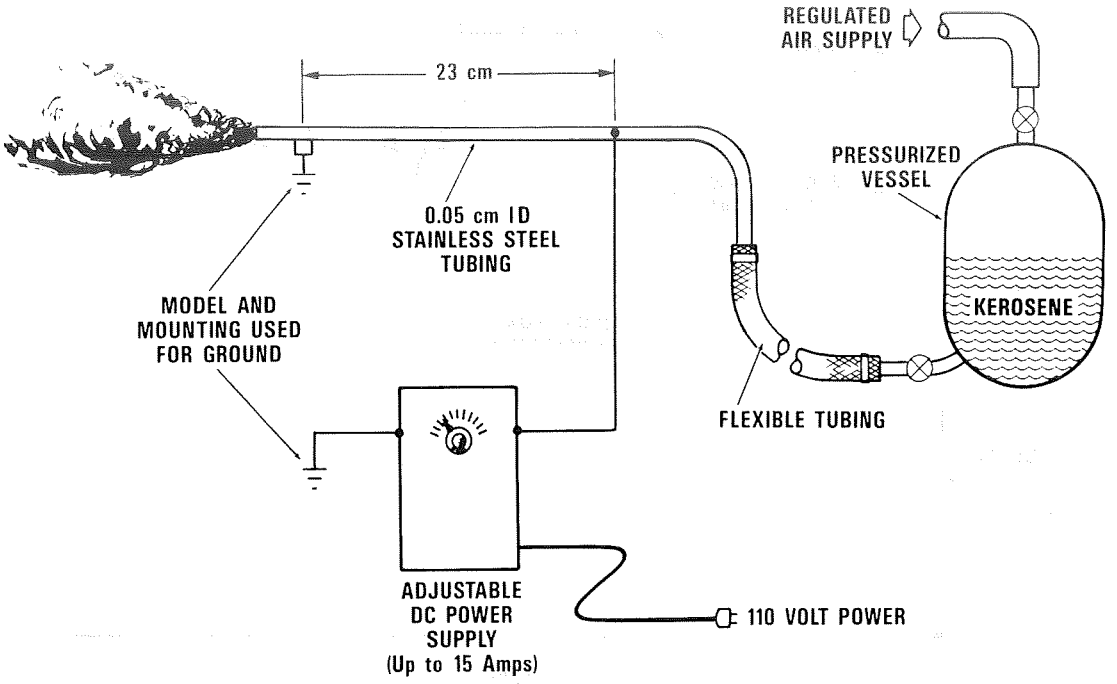

Figure 3 Schematic Diagram of the Smoke Generator.

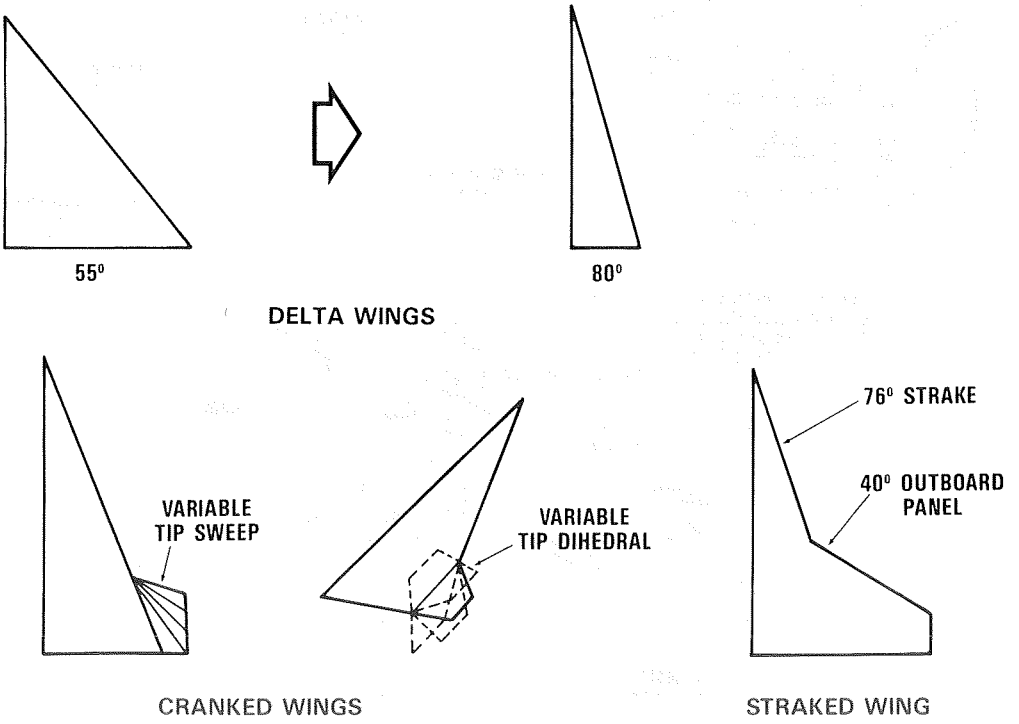

Figure 4 Semi-Span Planforms Tested.

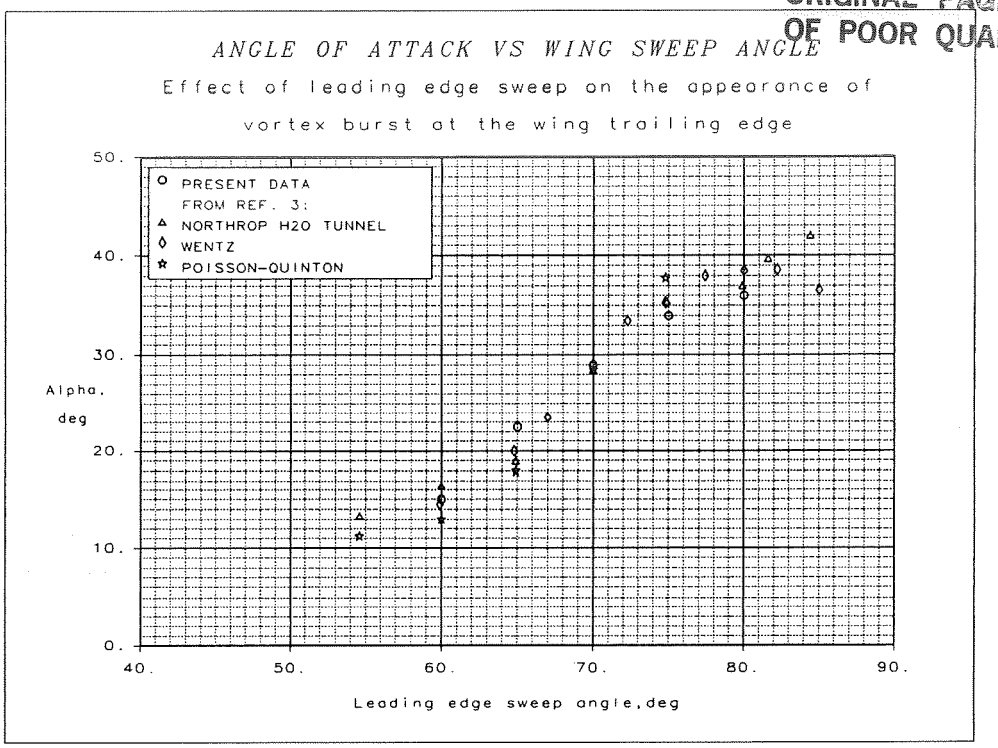

Figure 5 Effect of Wing Sweep on TE Vortex Burst.

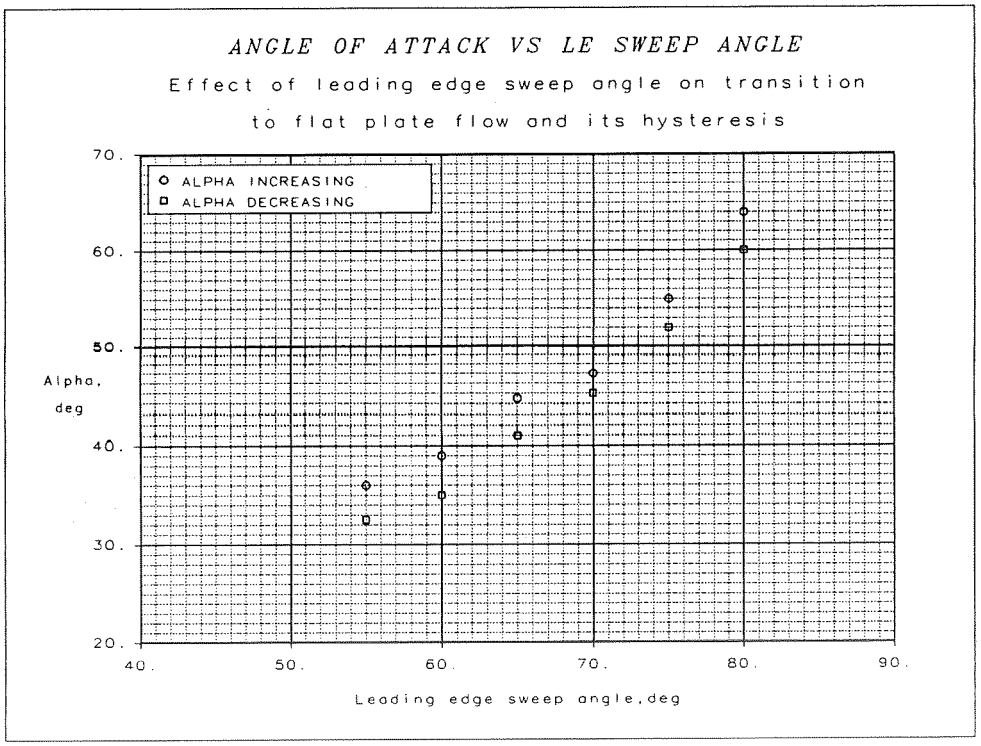

Figure 6 Effect of Wing Sweep on FP Flow Transition.

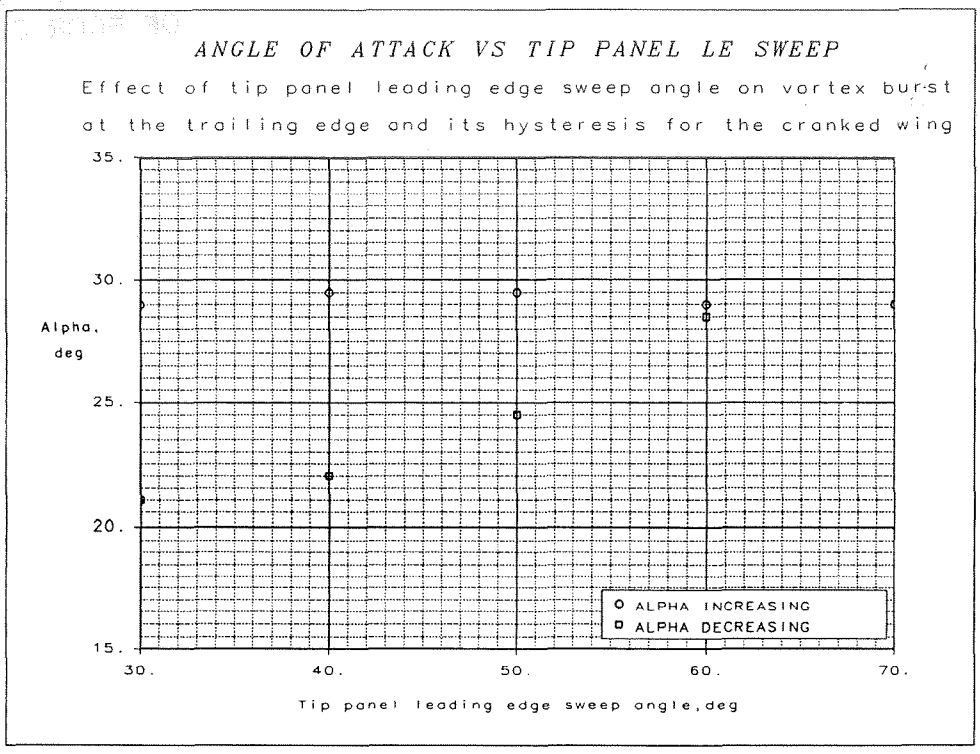

Figure 7 Effect of Tip Panel Sweep on TE Vortex Burst on Cranked Wings.

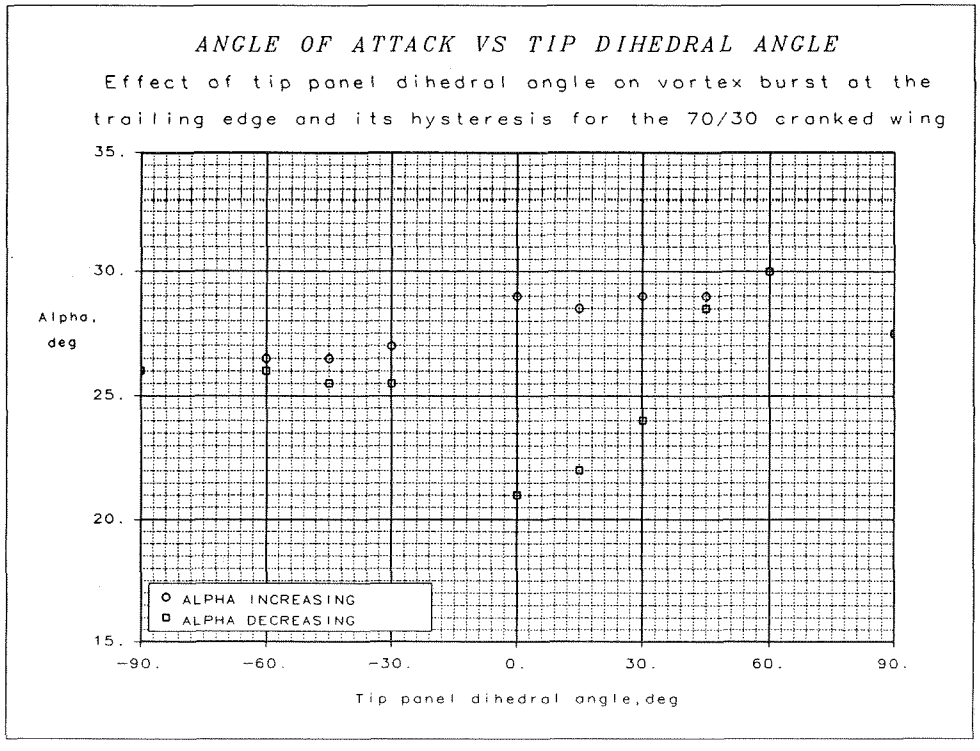

Figure 8 Effect of Tip Panel Dihedral on TE Vortex Burst on a 70°/30° Cranked Wing.

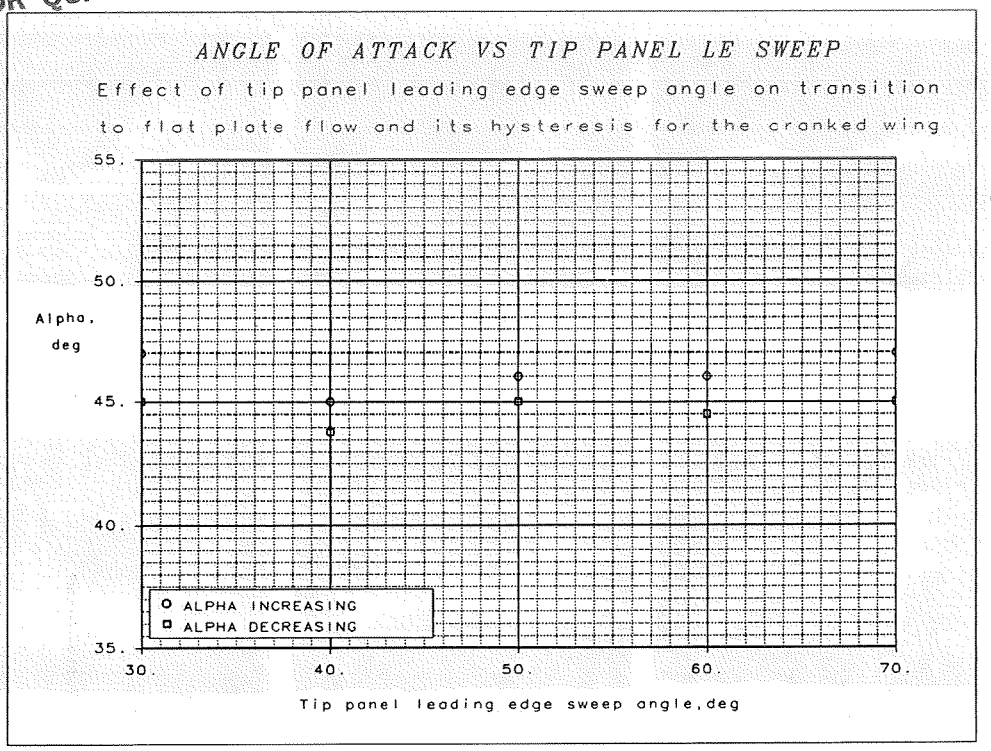

Figure 9 Effect of Tip Panel Sweep on FP Flow Transition on Cranked Wings.

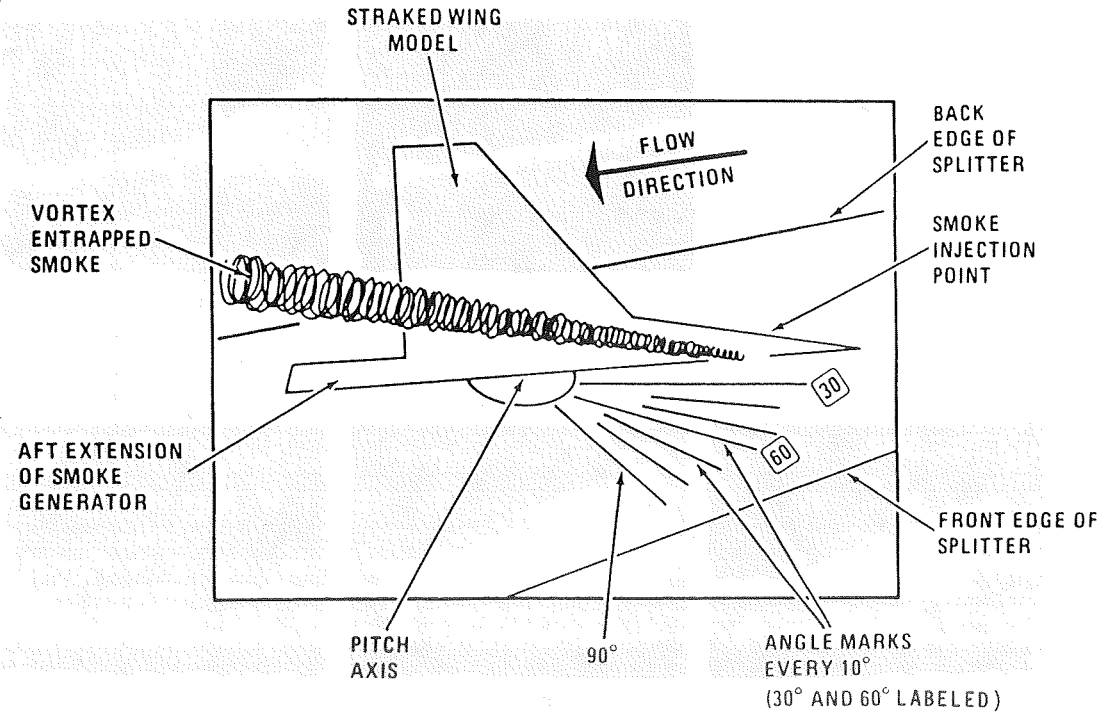

Figure 10 Explanation of Flow Visualization Results.

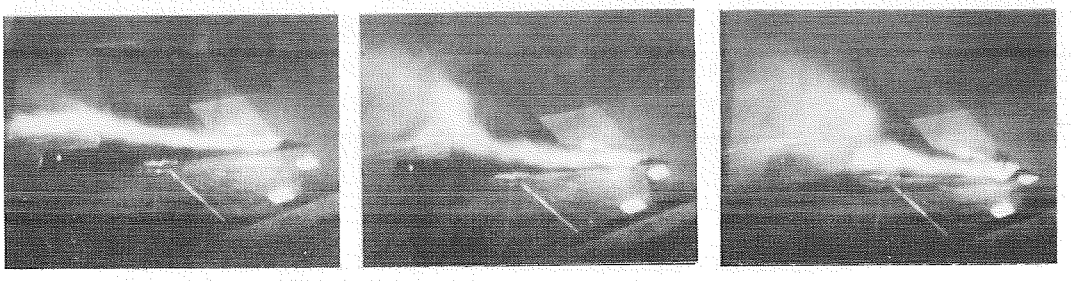

11 (a) $\alpha = 15^0$ 11 (b) $\alpha = 20^0$ 11 (c) $\alpha = 28^0$

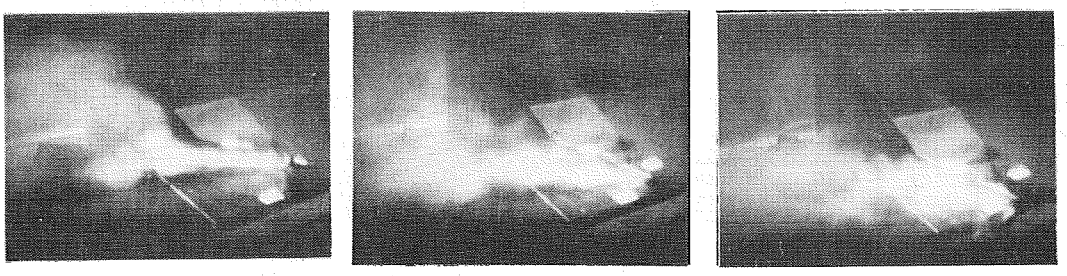

11 (d) $\alpha = 35^0$ 11 (e) $\alpha = 45^0$ 11 (f) $\alpha = 55^0$

Figure 11 Flow Visualization Results for the Straked Wing.

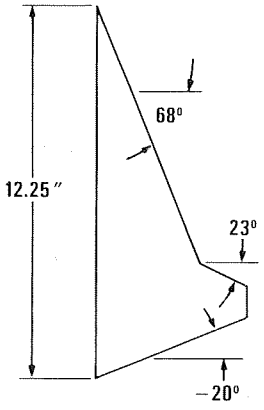

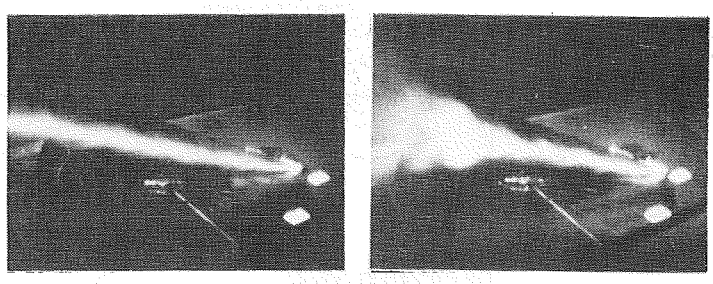

12 (a) $\alpha = 20^0$ 12 (b) $\alpha = 25^0$

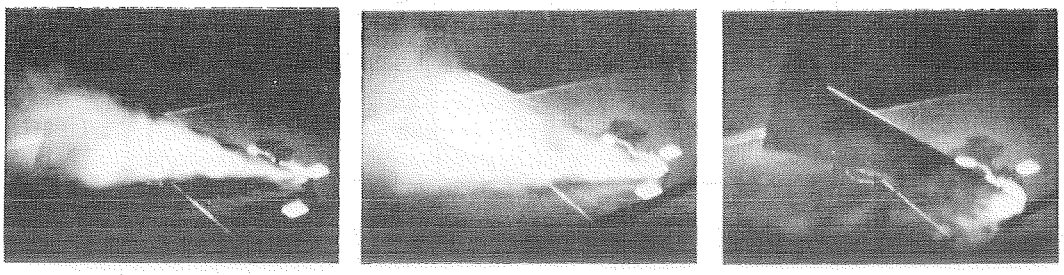

12 (c) $\alpha = 35^0$ 12 (d) 45° 12 (e) 55°

Figure 12 Flow Visualization Results for a Cranked Wing.